# Mechanochemically driven transformations in organotin chemistry: stereochemical rearrangement, redox behavior, and dispersion-stabilized complexes

Ross F. Koby[a], Timothy P. Hanusa*[a], and Nathan D. Schley[a]

Department of Chemistry, Vanderbilt University, VU Station B #351822, Nashville, Tennessee 37235

**ABSTRACT:** Ball milling a mixture of the bulky allyl K[A′] ([A′] = [1,3-$(SiMe_3)_2C_3H_3$]$^-$) and $SnCl_2$ in a 2:1 ratio for 5 min leads to the tris(allyl) stannate $[SnA'_3K]_\infty$, which forms a coordination polymer in the solid state. Longer grinding of the 2:1 mixture (15 min), or the use of a 3:1 ratio of reagents, initiates a disproportionation reaction and the chiral tetra(allyl)tin species $[SnA'_4]$ is produced. A small amount of a diastereomeric $[SnA'_4]$ complex with *meso* symmetry can also be isolated with extended grinding. These products have been structurally authenticated with single crystal X-ray crystallography. The tetra(allyl) species $[SnA'_4]$ are sterically crowded, and decompose relatively quickly (< 1 hr) in hydrocarbon solvents. In the solid state, they are much more persistent (several months), and evidently owe their stability to internal London dispersion interactions, as evidenced by multiple close H⋯H′ interligand contacts. Dispersion-corrected DFT calculations have been used to confirm the critical contribution of dispersion interactions to their stability. None of these products are available in their isolated forms from solution-based reactions, demonstrating the ability of mechanochemical activation to access otherwise unobtainable transformations in organotin chemistry.

## INTRODUCTION

Mechanochemistry, especially in the form of grinding and ball milling,[1] is a technique that has experienced a resurgence in modern preparative chemistry, encompassing the synthesis of organic,[2-4] organometallic,[5-9] and coordination compounds,[10-13] and the generation of new nanomaterials.[14-15] In most cases, reactions performed mechanochemically require little to no solvent, use less energy, and proceed more quickly than conventional solvent-based reactions. Besides being compatible with the philosophy and practice of green chemistry,[16-17] mechanochemistry can significantly alter reaction outcomes. Kinetics and mechanisms can be drastically changed,[3] providing access to new products in higher yields and shorter reaction times than otherwise possible.[4] Most intriguingly, mechanochemistry has been used to form a variety of organic and organometallic compounds not available through solution methods, revealing pathways to compounds that are unique to the solid state approach.

The reasons that mechanochemically promoted syntheses can differ from solution-based reactions are varied. For example, the solvents required to dissolve starting materials might also attack the product; this is the reason that only a mechanochemical approach was successful in producing the unsolvated tris(allyl) aluminum complex $[AlA'_3]$ ([A′] = [1,3-$(SiMe_3)_2C_3H_3$]$^-$) (Figure 1a).[5] Alternatively, usable solvents, even at their boiling points, may not provide enough energy input to overcome the reaction barrier preventing a molecule from being assembled, as with the sterically encumbered adamantoid phosphazane $P_4(N^tBu)_6$ (Figure 1b).[18] In a third case, owing to different reaction rates and effective concentrations of reagents, solution-based and mechanochemical reactions may reach different endpoints, as in the reaction of $C_{60}$ with KCN. In solution, the reaction stops with the hydrocyanation product $[C_{60}(CN)]^-$, whereas in the solid state, the cyano anion reacts with additional $C_{60}$ to form the fullerene dimer, $C_{120}$ (Figure 1c).[19,20] These examples do not exhaust the ways that solvent removal combined with mechanochemical activation can facilitate the synthesis of new compounds. We describe here the formation through mechanochemical synthesis of sterically bulky allyl compounds that exist because of a disproportionation reaction involving tin. The redox process is not observed when the reaction is conducted in solution.

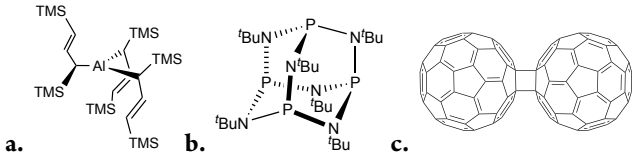


**Figure 1.** Compounds formed exclusively through mechanochemical methods: a. an unsolvated tris(allyl) complex, [Al{1,3-$(SiMe_3)_2C_3H_3$}$_3$];[5] b. a $^t$Bu-substituted phosphazane;[18] c. the fullerene dimer, $C_{120}$.[19,20]

It should be noted that many organotin(IV) species display considerable thermal, hydrolytic, and oxidative stability, which in general is a result of kinetic factors, and not especially strong Sn–C bonds.[21] The corresponding neutral tin(II) alkyl and aryl complexes (stannylenes, [:$SnR_2$]), in contrast, are generally more reactive, and unless stabilized with sterically bulky groups[22] or cyclopentadienyl ligands,[23] commonly occur only as transient reaction intermediates.[24] Sterically enhanced allyl ligands[25-27] have been used to suppress oligomerization and enhance kinetic stability in a wide range of metal complexes, and offer a way to generate stabilized tin(II) allyl species. Layfield explored the use of the trimethylsilylated allyl ligand A′ with tin, demonstrating that the reaction of 3 equiv of K[A′] with $SnCl_2$ in THF leads to the stannate $[SnA'_3K(thf)]$, in which the thf-coordinated potassium ion also interacts in a cation-π fashion

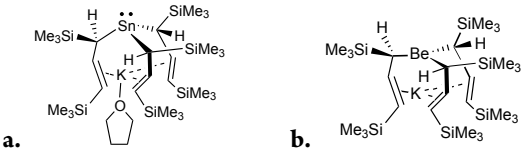


**Figure 2. a.** Schematic of $[SnA'_3K(thf)]$; the coordination around Sn is pyramidal, with the sum of C–Sn–C′ angles = 288.5°.[28] **b.** Schematic of $[BeA'_3K]$; Be is in a near planar environment, with the sum of C-Be-C′ angles = 357.6°.[29] Similar trigonal planar coordination is found in the $[ZnA'_3M]$ (M = Li, Na, K) complexes.[30]

with the double bonds of the three allyl ligands (Figure 2a).[28] The same structural motif is found in isostructural beryllium[29] and zinc[30] complexes (Figure 2b). These compounds have no counterparts with unsubstituted allyl ligands.

All the $[M^{II}A'_3M^{I}(thf)_n]$ metallates are found in a $C_3$-symmetric *R,R,R* (or *S,S,S*) configuration, with the stereodescriptors referring to the attachment site of the allyls to the metal centers. In contrast, the related neutral $MA'_3$ (M = As, Sb, Bi) complexes exist in two diastereomeric forms, with *R,R,R* (equivalently, *S,S,S*) and *R,R,S* (or *S,S,R*) arrangements.[31] It is likely that the alkali metal counterions in the anionic complexes serve to template the arrangement of the allyl ligands around the central element.[29]

## RESULTS

Even though the unsubstituted di(allyl)tin $[Sn(C_3H_5)_2]$ is unknown, it seemed possible that the use of only two equiv. of K[A′] and the avoidance of a coordinating reaction solvent could lead to the isolation of the substituted analogue, $[SnA'_2]$.[32] As a check to ensure that mechanochemical activation was actually needed, stirring a mixture of K[A′] and $SnCl_2$ in hexanes produced no reaction, but grinding the same solids together in a 2:1 ratio for 5 min in a planetary ball mill generated a brown powder that was partially hexanes-soluble. Filtration of a hexanes extract to remove insoluble matter, evaporation of the filtrate, and subsequent crystallization from hexanes led to the isolation of canary yellow crystals of **1**, whose $^1$H NMR spectrum shows 5 resonances characteristic of σ-bound A′ ligands (2 singlets for the trimethylsilyl groups and 3 allylic signals; details in the SI). This data and the observation of a singlet in the $^{119}$Sn NMR spectrum at δ -138.7 ppm, not far from the δ -132.9 ppm resonance reported for $[SnA'_3K(thf)]$,[28] suggested that a similar structure might be involved, despite the suboptimal ratio of reagents in the mechanochemical reaction. It should be noted that **1** is evidently the most stable (and the most easily generated) product of the K[A′]:$SnCl_2$ system, as it can be formed under a range of mechanochemical conditions, including changes of scale and reaction stoichiometry (from 1:1 to 5:1), although its purity and yield varies with the specific reaction parameters used (additional examples in the SI).

A single crystal X-ray structure of **1** revealed that the compound was in fact the stannate $[SnA'_3K]$, with three σ-bound allyls ligands on tin and the $K^+$ counterion coordinated to the π-bonds of the allyl ligand (Figure 3). The core structure, with its $\mu:\eta^2:\eta^1$-bonding arrangement to K and Sn, is thus isostructural with the thf-solvated Sn species, and with the Zn and Be counterparts. Owing to the lack of coordinated thf in **1**, the $K^+$ is located more deeply inside the 'umbrella' formed by the three allyl ligands than is the case in the thf-solvated species. This is reflected in the $K^+\cdots Sn$ separation of 3.537(1) Å in **1**, notably shorter than the corresponding 3.666(3) Å distance in the solvate.[28] As a result, two of the α-carbons are found at the same distances from the $K^+$ (3.01, 3.07 Å) as are the olefinic carbons (average distance of 3.06 Å), even though the α-carbons are saturated and not similarly basic. The $[SnA'_3]^-$ framework distorts enough that the third $K^+\cdots\alpha$ carbon contact ($K^+\cdots C10$) is moved away to 3.20 Å.

A notable difference of **1** from its Be, Zn, and solvated-Sn precedents is that it exists in the solid state as a coordination polymer, with the $K^+$ ion interacting with a methyl group on a neighboring molecule at a distance of 3.198(8) Å. This distance is about 0.1 Å longer than that of $K^+$ to the olefinic carbons of the allyl groups, but it is similar to the $K^+\cdots CH_3$ linkage found in the coordination polymer $[K(18\text{-}C\text{-}6)SnMe_3]_\infty$ (3.181(3) Å), for example, or in the discrete anion $[(Me_2SnCH_3)K(18\text{-}c\text{-}6)SnMe_3]^-$ anion (3.237(2) Å).[33] DFT calculations on the latter provided a $K^+\cdots CH_3$ force constant ($k$) of 16-17 N m$^{-1}$, in the range of hydrogen bonds.[33] The unit cell of **1** ($P2_1/n$, $Z = 4$) comprises parts of two chains; all of the stannate units in a single chain possess the same arrangement of allyl ligands around the tin (*R,R,R*, or *S,S,S*, with the latter shown in Figure 3). The other chain displays the opposite configuration, so that a racemic mixture of chains is present.

The weakness of the intermolecular interaction in **1** explains its facile disruption, as happens from the presence of the coordinated thf ligand in $[SnA'_3K(thf)]$.[28] The ease of such disruption was also demonstrated from one particular recrystallization attempt of **1**, in which trace adventitious water, evidently from the solvent, was found to be bound to the $K^+$ ion, interrupting the $K^+\cdots CH_3$ linkage and converting the stannate into discrete solvated monomers, $[SnA'_3K(OH_2)]$, **2** (Figure 4). The near absence of other evidence of hydrolysis products (e.g., HA′ in $^1$H NMR) is a testament to the minute amount of water involved, the greater Lewis acidity of $K^+$ relative to the tin center, and to the relatively low polarity of the Sn–C bonds. Like $[SnA'_3K(thf)]$, **2** has crystallographically imposed 3-fold symmetry (the H atoms on water are disordered), and the water is associated with an increase in the effective coordination number of $K^+$. The average distance of the $K^+$ to the olefinic carbons lengthens from 3.06 Å in **1** to 3.13 Å in **2**, a change that tracks with the difference between the ionic radii of 6- and 7-coordinate $K^+$ (0.08 Å).[34]

The possibility that the unsolvated **1** might be usable as a 6-e$^-$ donor ligand, isoelectronic with $Cp^-$, and a tripodal synthon for heterobimetallic allyl complexes[28] prompted a more thorough examination of its preparation. As a first step, the reagent stoichiometry of K[A′] and $SnCl_2$ was

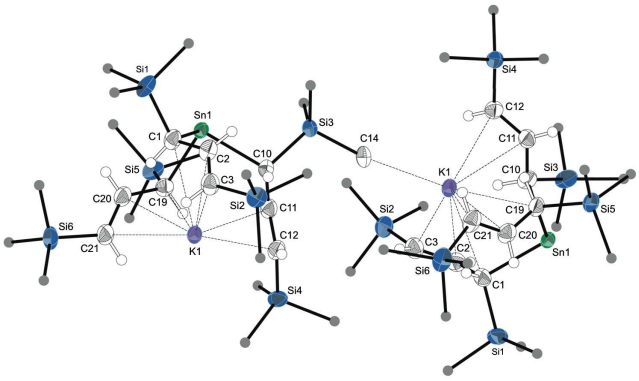


**Figure 3.** Thermal ellipsoid plot (50% level) of two molecules of **1**. For clarity, hydrogens have been removed from trimethylsilyl groups, and with the exception of C14, their carbon atoms have been replaced with grey circles. Selected bond distances (Å) and angles (deg): Sn1–C1: 2.324(5); Sn1–C10: 2.346(5); Sn1–C19: 2.310(5); K1–C1: 3.073(7); K1–C2: 3.090(6); K1–C3: 2.979(6); K1–C10: 3.204(5); K1–C11: 3.126(5); K1–C12: 3.007(5); K1–C19: 3.010(6); K1–C20: 3.069(6); K1–C21: 3.062(5); K1$\cdots$C14: 3.198(8); C1–Sn1–C10: 97.47(19); C1–Sn1–C19: 96.77(19); C10–Sn1–C19: 95.45(18).

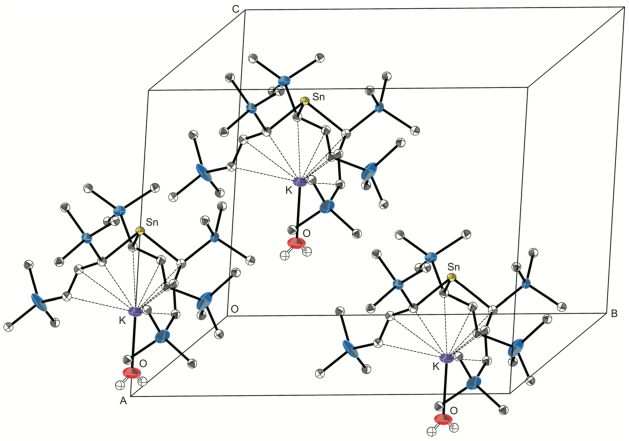


**Figure 4.** Thermal ellipsoid plot (50% level) of the unit cell of **2** (space group *R*3*m*, *Z* = 3). For clarity, all hydrogens have been removed except from the water molecules, and carbon atoms have been assigned arbitrary isotropic radii. Crystallographically imposed disorder in the allyl ligands has also been removed. Selected bond distances (Å) and angles (deg): Sn–C: 2.338(7); K–O: 2.729(14); K···C: 3.09–3.17 Å; C–Sn–C′: 96.6(2).

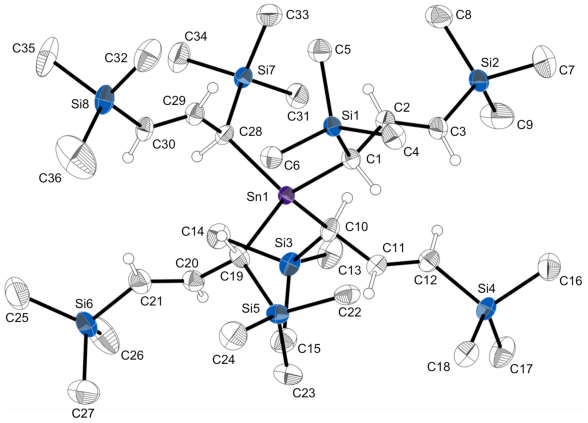


**Figure 5.** Thermal ellipsoid plot (50% level) of **3**. For clarity, hydrogens have been removed from trimethylsilyl groups, and the others assigned an arbitrary radius. Selected bond distances (Å) and angles (deg): Sn1–C1: 2.195(6); Sn1–C11: 2.203(5); Sn1–C19: 2.206(5); Sn1–C28: 2.195(6); C1–C2:1.493(8); C2–C3: 1.337(8); C10–C11: 1.490(8); C10–C11: 1.490(8); C19–C20:1.495(10); C20–C21: 1.334(9); C28–C29: 1.484(8); C29–C30: 1.333(9); C1–Sn1–C10: 105.2(2); C1–Sn1–C19: 110.0(3); C1–Sn1–C28: 112.7(2); Sn1–C1–C2–C3: 111.5(5); Sn1–C10–C11–C12: 126.4(4); Sn1–C19–C20–C21: 123.6(5); Sn1–C28–C29–C30: 101.7(5).

adjusted from 2:1 to 3:1, in order to improve the yield of the original reaction; this was also the ratio originally used to produce [SnA′$_3$K(thf)] in THF.[28] Now, however, milling the two reagents for 5 min left an oily residue. Extracting the solid with hexanes left an insoluble heterogeneous mixture of a light bluish-grey and dark grey powder, assigned to potassium chloride and tin metal, respectively.[35] Filtration of the hexanes extract followed by removal of solvent from the filtrate left a beige solid (**3**). It quickly became evident that **3** was a substance considerably different from the intended **1**.

A striking feature of **3** is its instability in solution. In the solid state at room temperature under an inert atmosphere, **3** is sufficiently stable to obtain combustion analysis and confirm the bulk purity of the freshly prepared material. Even a 6-month old sample was only partially decomposed, and contained crystals of satisfactory quality to allow a redetermination of its X-ray structure (see below). However, when dissolved in hexanes, only about an hour of working time is available before visible decomposition is evident, which is accompanied by the formation of a precipitate. One of the species present in the aged solution is tetrakis(trimethylsilyl)-1,5-hexadiene {A′$_2$}, a product of allyl radical coupling.[36] Nevertheless, rapid recrystallization is possible from freshly prepared hexanes solutions, and although crystals suitable for X-ray analysis could be obtained this way (see below), such attempts often resulted in the formation of oily solids. Dissolved in $C_6D_6$ at room temperature for the purpose of NMR studies, the onset of decomposition is even more rapid, with the initial amber solution beginning to turn brown after ca. 10 min, and eventually yielding a dark precipitate. This had the consequence of making clean NMR spectra difficult to obtain. Even with the additional step of freezing the sample in liquid nitrogen immediately after preparation, and thawing it just before signal collection, decomposition products were invariably detectable in NMR spectra.

Despite difficulties with sample stability, a $^{119}$Sn NMR spectrum of **3** was eventually obtained that displayed a single peak at δ -36.6 ppm, a roughly 100 ppm downfield shift from that for [SnA′$_3$K]. If all else were equal, the decrease in shielding would suggest a reduction in metal coordination number, but given the broad chemical shift range for $^{119}$Sn in complexes with hydrocarbyl ligands (over 1000 ppm),[37] and the high sensitivity of the shift to minor structural changes, this alone was not diagnostic of the structural differences from [SnA′$_3$K]. The $^1$H NMR spectrum contains resonances consistent with σ-bonded allyl ligands, but these are also not determinative of structure. The identity of **3** was eventually established from the results of a single crystal X-ray study, performed on a crystal obtained from a rapidly evaporated hexanes solution. It proved to be the tetra(allyl)tin(IV) complex, [SnA′$_4$] (Figure 5), which represents the first crystal structure of a homoleptic tin allyl complex. Its formation, discussed below, also represents the first example of a mechanochemically driven organometallic disproportionation reaction, occurring without the benefit of added external oxidants.[38-39]

Around the central tin atom of **3**, four σ-bound allyls are arranged in a distorted tetrahedral fashion, all of which are attached with the same relative stereochemistry, generating a chiral center. (In the crystal selected for analysis, the orientation is *S*,*S*,*S*,*S*, although under a microscope with polarizing filters, crystals that rotated light with the opposite orientation were also observed.) The combined effect is to give the molecule approximate $D_2$ symmetry, although this is not crystallographically imposed. The average Sn–C bond length of 2.200(11) Å is on the long end of known Sn-C(allyl) distances in Sn(IV) compounds, but is similar to that found for the Sn–allyl bond in the trimethylsilylated compound $Sn(CH_2Ph)_2[C(SiMe_3)_3][CH_2CH{=}C(SiMe_3)_2]$ (2.19(1) Å).[40] The Sn-C-C=C torsion angles range from 101.7° to 126.4°, averaging to 115.8°. The angles are larger than typical values observed in Sn-allyl compounds (100±10°, see below), but they can be influenced by steric crowding (the value in $Sn(CH_2Ph)_2[C(SiMe_3)_3][CH_2CH{=}C(SiMe_3)_2]$ is 128.5°).[40]

To gain further insight into the origins of both **1** and **3**, both of which involve substoichiometric ratios of reagents, a wider range of reagent ratios and grinding times (up to 60 min) was studied. With a 2:1 ratio of K[A′]:$SnCl_2$ and a 15 min grinding time, a more complex mixture of products was observed, including **1**, **3**, and a small amount of a new substance (**4**) that displayed a single peak in its

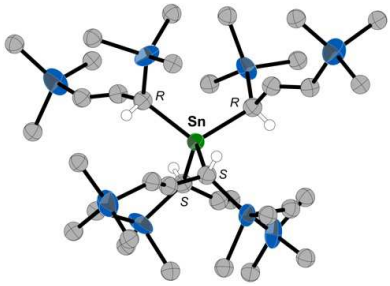


**Figure 6.** Connectivity of **4**. Thermal ellipsoids of Sn and Si are at 50% probability; carbon atoms are given arbitrary radii, and all hydrogens have been removed except for those required to illustrate the stereochemistry at the α-carbon positions.

$^{119}$Sn NMR spectrum at δ -32.5 ppm, close to but distinctly different from the δ -36.6 ppm shift for **3**. It yielded crystals following the standard workup with hexanes, but the best X-ray diffraction data that could be obtained was from a crystal that proved to be twinned and from which almost no high angle information was obtained, so that the resulting structure was essentially of connectivity only quality. Nevertheless, the space group ($P\bar{1}$, $Z = 2$) was clearly different from that for **3** ($P2_1$), and the heavy atom connectively is not in doubt. It proved to be a diastereomer of **3**; specifically, the connectivity of the allyl ligands to the tin has *R*,*S*,*R*,*S* stereochemistry, so that the molecule has *meso* symmetry (Figure 6). The idealized symmetry of **4** is $S_4$, rather than the $D_2$ of **3**.

Milling the 3:1 mixture of starting materials for 15 min led to a mixture similar to that observed with the 2:1 ratio; i.e., not only was **3** present, but also **1**, **4**, and K[A′]. Extending the grinding time to 60 min did not reveal any other identifiable tin-containing species (search conducted from δ +500 to -2000 ppm).

## DISCUSSION

Determining the course of mechanochemically activated reactions is challenging, and although substantial progress has been made in recent years by employing synchrotron radiation[41-43] or ex-situ Raman spectroscopy,[44-47] such experimental set-ups are not yet common or universally applicable.[48-49] In the present case, despite the complex interrelationships between the various compounds produced from $SnCl_2$ with K[A′], a plausible scheme for the reactions with a 2:1 ratio of reagents that captures the non-stoichiometric origin of the compounds can be constructed (Scheme 1). The non-stoichiometric formation of **1** and **3** has precedent in beryllium chemistry, where [KBeA′$_3$] is formed from the milling of a 2:1 mixture of K[A′] and $BeCl_2$.[29] There is also related non-stoichiometric behavior known in (solution-based) tin chemistry, as the reaction of a 3:1 ratio of Li[$^i$Pr] and $SnCl_4$ does not produce the expected [Sn$^i$Pr$_3$Cl], but rather gives rise to a mixture of [Sn$^i$Pr$_4$], [Sn$^i$PrCl$_3$], and [Sn$^i$Pr$_2$Cl$_2$] in roughly equal amounts.[50] The rapid formation of **1** is also paralleled in the formation of [KBeA′$_3$], which is assembled within 15 min of the start of milling. The slower conversion of the starting materials into **3** and **4** is understandable based on the need for redox reactions to intervene and the ensuing steric congestion around the metal center.

Computational investigations were performed to provide insight into the properties of **3** and its relationship to **1** and **4**. DFT calculations were conducted with the B3PW91 hybrid functional[51] with additional dispersion correction provided by Grimme's D3 dispersion correction[52] and Becke-Johnson dampening (D3-BJ)[53] (see computational details in the SI).

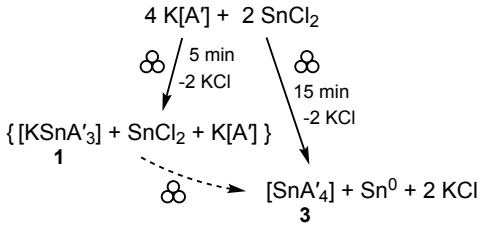


**Scheme 1.** Possible formation of **1** and **3** from a 2:1 ratio of K[A′] and $SnCl_2$.

**Instability of [SnA′$_4$].** The solution instability of **3** was unanticipated, as the parent tetra(allyl)tin is an air- and $H_2O$-stable oil, bp 87–88 °C/4 mmHg,[54] and the addition of trimethylsilyl groups to the allyl ligands was, if anything, expected to enhance the stability of the complex. It has of course long been known that organotin complexes with unsaturated ligands (e.g., vinyl, phenyl, allyl) are more labile than the corresponding saturated counterparts, which is the source of their usefulness in synthetic chemistry.[55] In particular, the R$_3$Sn–allyl bond has been estimated as being ca. 10 kcal mol$^{-1}$ weaker than an analogous R$_3$Sn–alkyl bond, although this number has not been experimentally verified.[56] The source of the weakening has been assigned to the so-called β-tin effect, which involves a hyperconjugative interaction between $\sigma_{M\text{-}X}$ and $(\pi_{C=C})^*$ orbitals.[57-60] This effect is maximized when the Sn–allyl bond is roughly orthogonal to the plane of the C=C group (in practice, the Sn-C-C=C torsional angle is usually found to be in the range of 100±10°). The delocalization of the π-electrons has the consequence of weakening the Sn–C(allyl) and C=C bonds, and greatly elevating the reactivity of allylstannanes with electrophiles. A simplified depiction of the interaction is provided in Figure 7a,b. A semi-quantitative indication of the bonding changes is reflected in the Mayer bond orders[61-62] for the model complex [Me$_3$Sn–A′] (Figure 7c). Whereas the Sn–C(methyl) bond orders are all close to unity (average value of 1.02), that for Sn–C(A′) is 0.81, a 20% decrease. The formal double bond of the allyl ligand is weakened slightly (BO = 1.78), although the BO of the formal C–C single bond does not reflect any strengthening (0.98). Despite these changes in bond strength, something more than the normal β-tin effect must be contributing to the extreme lability of **3**.

A series of calculations was completed to determine whether there were special consequences associated with the hyperconjugation in **3**, beginning with a calibration on the energy of methyl group dissociation from $SnMe_4$ ($SnMe_4 \rightarrow \bullet SnMe_3 + \bullet Me$), for which an experimental value is available ($\Delta H° = 69\pm2$ kcal mol$^{-1}$;[63] note that this number is for the first methyl group cleavage, not the mean bond dissociation enthalpy, $\bar{D}$(Sn–C).[64] The calculated value, 69.0 kcal

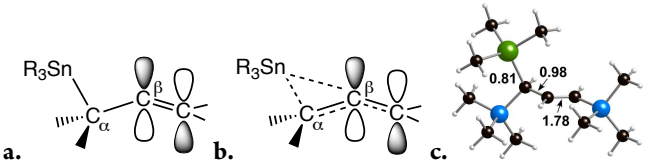


**Figure 7.** Consequences of hyperconjugative interaction of $\sigma_{Sn\text{-}X}$ and $(\pi_{C=C})^*$ orbitals in allyl-tin species. **a**. The formal bonding arrangement without hyperconjugation. **b**. The Sn–C(allyl) and C=C bonds are weakened. **c**. Mayer bond orders in the allyl ligand of [Me$_3$Sn–A′] (green = Sn; blue = Si).

mol$^{-1}$ ($\Delta H°$), is in excellent agreement with the experimental figure (Table 1, no. 1). The free energy of dissociation is about 12 kcal mol$^{-1}$ lower than this. For the more relevant reaction involving tetra(allyl)tin (i.e., $Sn(C_3H_5)_4 \rightarrow \bullet Sn(C_3H_5)_3 + \bullet C_3H_5$), both the enthalpy and free energy of dissociation are lowered relative to tetramethyltin (no. 2). Notably, the $\Delta G°$ value is 16.2 kcal mol$^{-1}$ less, reflecting a bond weakening consistent with the operation of the β-tin effect.

Adding silyl ($SiH_3$) groups to the 1- and 3-positions of the allyls leaves the free energy of dissociation essentially unaffected compared to the unsubstituted allyl (Table 1, no. 3). For the full model of **3** ($SnA'_4 \rightarrow \bullet SnA'_3 + \bullet A'$), however, the free energy value actually *increases* by 12 kcal mol$^{-1}$ (Table 1, no. 4), a result that was initially unexpected in view of the substantial increase in the steric bulk of the ligands, and the anticipated bond weakening that would occur through interligand Pauli repulsion.

The steric congestion that is present in **3** and **4** can be visualized in the encapsulation of the metal coordination sphere. As estimated with the program Solid-G,[65] and specifically by the value of $G_{complex}$, the net percentage of coordination sphere covered by the ligands, the value for $[SnMe_4]$ is low (60.5%), and increases only to 69.7% for $[Sn(C_3H_5)_4]$ (Figure 8a). For **3** and **4**, however, the $G_{complex}$ values rise to 97.1% and 96.2%, respectively (Figure 8b,c).[66]

A counteracting consequence of the proximity of the many $SiMe_3$ groups is that they can serve to stabilize the molecule through the operation of London dispersion forces (LDF). The ability of bulky groups such as *t*-butyl or $SiMe_3$ to function as "dispensers" of attractive dispersion energy, and not simply as centers of repulsive force, has been computationally demonstrated by Grimme,[67] and used to explain the stability of the heavily substituted hexakis(3,5-di-*t*-butylphenyl)ethane,[68] even though the ostensibly less crowded parent molecule hexaphenylethane cannot be isolated.[69] It has now been recognized that a range of inorganic and organometallic molecules owe their existence to the operation of LDF provided by groups such as terphenyl, $-C(SiMe_3)_3$, $[-N(SiMe_3)_2]^-$, and norbornyl.[70]

One of the distinctive structural markers of these LDF-stabilized molecules is the presence of multiple interligand H···H′ contacts that are at or below the sum of the van der Walls radii ($2r_H$ = 2.40 Å).[71] Not surprisingly, both **3** and **4** display numerous such contacts (Figure 9), and significantly, there are no analogous distances in the calculated structures of $[Sn(C_3H_5)_4]$ or $[Sn\{(1,3\text{-}SiH_3)_2C_3H_3)\}_4]$.

Computational support for the importance of LDF in stabilizing **3** was gathered by examining the dissociation reaction ($SnA'_4 \rightarrow \bullet SnA'_3 + \bullet A'$) without explicit dispersion corrections, i.e., using only the unmodified B3PW91 functional (Table 1, no 5). Both $\Delta H°$ and $\Delta G°$ fall by 42%, and are well below the values found for the complex with $SiH_3$-substituted allyls. This both quantifies the role that LDF plays in stabilizing the molecules, and indicates that the $-SiMe_3$ groups would in fact be weakening the bonding owing to steric repulsions if the dispersion forces were not opposing their effects.

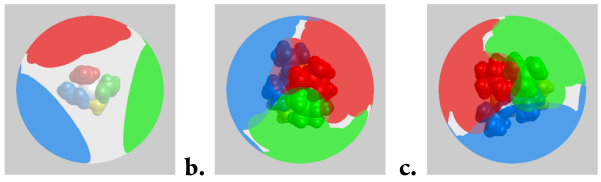


**Figure 8.** Visualization of the extent of coordination sphere coverage ($G_{complex}$) of: (a) $[Sn(C_3H_5)_4]$, 69.7%; (b) **3** ($D_2$ symmetry), 97.1%; (c) **4** ($S_4$ symmetry), 96.2%. Optimized coordinates (B3PW91-D3BJ/def2-TZVP(Sn,Si),def2-SVP(C,H)) and the program Solid-G[39] were used. The $G_{complex}$ value represents the net coverage, so that regions of the coordination sphere where the projections of the ligands overlap are counted only once.

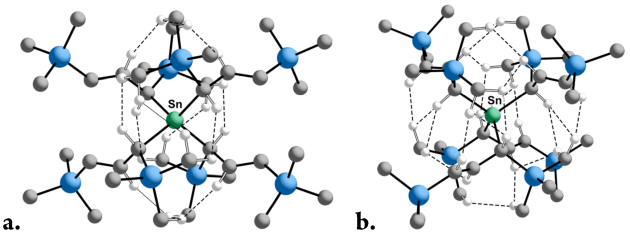


**Figure 9.** Frameworks of **3** (a) and **4** (b), illustrating H···H′ contacts that are less than the sum of the van der Waals' radii (≤ 2.4 Å). The contacts range from 2.07–2.30 Å in **3**, and from 2.01–2.29 Å in **4**. Contacts are calculated from the geometry optimized structures; for contacts from the X-ray data of **3**, see the SI.

Solvent interactions, even from alkanes, can interfere with the action of LDFs,[69] and cyclohexane was found to do so with hexakis(3,5-di-*t*-butylphenyl)ethane to the extent that $\bullet C_6H_3(3,5\text{-}^tBu)_2$ radicals are formed in solution.[69] It is appears that that hexanes and toluene exert the same effect on **3**, accounting for its rapid degradation in solution. The presence of $\{A'_2\}$ in the solution spectra of **3** is consistent with the disruption of the interligand LDF and the release of •A′ radicals, followed by their subsequent coupling.

**Formation of $[SnA'_4]$.** Starting from $SnCl_2$ and K[A′], the formation of **3** and **4** obviously involves multiple steps, including the stereoregular assembly of the ligands around the metal and the oxidation of Sn(II) to Sn(IV). It is most likely that the stannate **1** is the precursor to the tetra(allyl)tins (see below), yet given the low yields of **3** (ca. 20%), we considered the possibility that it is formed independently of **1**. That is, some of the unreacted $SnCl_2$ remaining after the formation of **1** (see the products of the 5 min grind in Scheme 1) could potentially undergo disproportionation to elemental tin and $SnCl_4$, with the latter then reacting with the residual K[A′] to form **3**. Using standard thermodynamic values,[72] the reaction in equation 1 is in fact slightly favourable.

$$2SnCl_2(s) \rightarrow SnCl_4(l) + Sn(s), \quad \Delta G° = -5.6 \text{ kcal mol}^{-1} \qquad (1)$$

This reaction can occur thermally, but at most to the extent of ca. 10%, and then only above temperatures of 500 °C.[73] In test grinds of

**Table 1.** Energies of ligand dissociation (B3PW91-D3BJ, kcal mol$^{-1}$)

| No. | Reaction[a] | Energy ($\Delta H°$, $\Delta G°$) |
|---|---|---|
| 1 | $SnMe_4 \rightarrow \bullet SnMe_3 + \bullet CH_3$ | +69.0[a], +56.9 |
| 2 | $Sn(C_3H_5)_4 \rightarrow \bullet Sn(C_3H_5)_3 + \bullet C_3H_5$ | +53.0, +40.7 |
| 3 | $Sn[(1,3\text{-}SiH_3)_2C_3H_3)]_4 \rightarrow \bullet Sn[(1,3\text{-}SiH_3)_2C_3H_3)]_3 + \bullet(1,3\text{-}SiH_3)_2C_3H_3$ | +59.7, +40.9 |
| 4 | $SnA'_4\ (D_2) \rightarrow \bullet SnA'_3 + \bullet A'$ | +70.6, +52.9 |
| 5 | $SnA'_4\ (D_2) \rightarrow \bullet SnA'_3 + \bullet A'$ | +41.1, +30.9[b] |

[a]Experimental value ($\Delta H°$) = 69±2 kcal mol$^{-1}$.[63] [b]Both $\Delta H°$ and $\Delta G°$ are calculated without dispersion corrections.

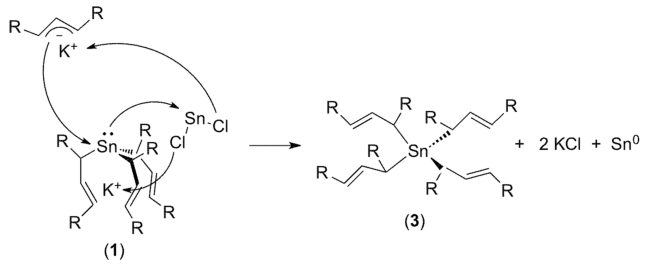


**Scheme 2.** Proposed formation of **3** from **1**. R = $SiMe_3$. This is a schematic to account for the reconnection of the various molecular fragments, not a detailed mechanism.

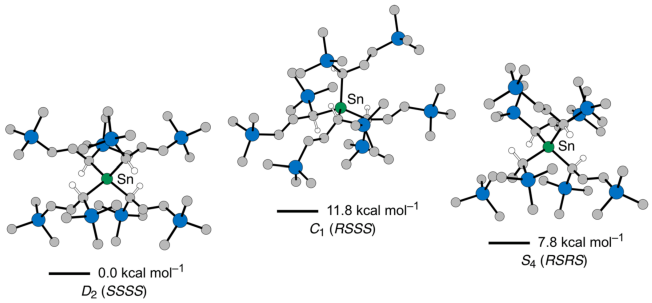


**Figure 10.** Relative energies of **3**, a nonsymmetric intermediate, and **4**, with conformations of (*S*,*S*,*S*,*S*), (*R*,*S*,*S*,*S*), and (*R*,*S*,*R*,*S*), respectively. Geometries were calculated at the B3PW91-D3BJ/def2-TZVP(Sn,Si), def2-SVP(C,H) level.

of $SnCl_2$ alone (with times up to 2 hours at 600 rpm in a planetary mill under $N_2$), we found no evidence for the formation of $SnCl_4$, suggesting that the reaction is kinetically inhibited.[74] Since the testing conditions were considerably more energetic than those present during the formation of **3**, it seems safe to discount this route as the source of Sn(IV). It is consequently much more likely that the tin that becomes oxidized is that in the stannate itself, given that the tin center is more electron rich in **1** than in $SnCl_2$, and that the stereochemical attachment is already set for the three allyl ligands. Only a single ligand needs to attach in the same conformation as the first three to generate **3**. The interchange of the ligands and electron transfer is sketched in a schematic (Scheme 2).

Compound **4** never appears apart from **3**, and then only at longer grinding times, suggesting that its formation is more difficult and takes additional steps. To compare the two energetically, both **3** and **4** were optimized under their idealized symmetry, i.e., $D_2$ and $S_4$, respectively. At the level of theory employed here, both are minima on their respective potential energy surfaces, and **4** is higher in energy by 7.8 kcal $mol^{-1}$ ($\Delta G°$). This is consistent with the faster formation of **3**, but also speaks to the more complicated route required to synthesize **4**. Formation of **4** from **3** would require a loss of two allyl ligands and their reattachment with the opposite stereoconfiguration. Starting with **3** with a (*S*,*S*,*S*,*S*) configuration, for example, loss of a ligand and then reattachment with inverted stereochemistry would lead to an (*R*,*S*,*S*,*S*) intermediate, found to be 11.8 kcal $mol^{-1}$ higher in energy than **3**. Repetition of the process with another *S*-bound allyl would generate the $S_4$ form, 4.0 kcal $mol^{-1}$ ($\Delta G°$) lower in energy than the intermediate. The three relevant forms are compared in Figure 10.

## CONCLUSIONS

In summary, we have demonstrated that the non-stoichiometric reactions observed in beryllium and zinc chemistry with a sterically bulky allyl ligand occur also with tin under mechanochemical conditions, producing a stannate, [$SnA'_3K$], from a 2:1 mixture of the potassium allyl K[A′] and $SnCl_2$. Furthermore, extended grinding initiates a redox reaction, from which tetra(allyl)tins, in both chiral and *meso* forms, can be isolated. The work demonstrates that even in the absence of solvent, stereochemical control can be maintained during the assembly of compounds, from the *R*,*R*,*R*/*S*,*S*,*S* chains of the allyl stannate, to the fully *R*,*R*,*R*,*R*/*S*,*S*,*S*,*S* forms of the tetra(allyl)tin [$SnA'_4$]. Both **3** and **4** evidently owe their solid-state stability to the operation of London dispersion forces provided by their $SiMe_3$ groups, which compensate for their otherwise sterically congested ligand environments. Considering that neither the unsolvated stannate **1** nor the solution-unstable tetra(allyl)tins are isolable from solvent-based reactions, these results exemplify unique characteristics of mechanochemical activation. A high probability exists that related transformative organometallic chemistry is to be found with other redox-active elements.

## CONFLICTS OF INTEREST

There are no conflicts to declare.

## ■ ASSOCIATED CONTENT

### Supporting Information

The Supporting Information is available free of charge on the ACS Publications website. Experimental (including NMR spectra) and computational details (PDF); optimized coordinates of all structures (.xyz format), and crystal data and summary of X–ray data collection for compounds **1**–**4**. Crystallographic data for the structures reported in this paper have been deposited with the Cambridge Crystallographic Data Centre as CCDC 1857435 (**1**), 1857436 (**2**), 1857437 (**3**), and 1857438 (**4**). Copies of the data can be obtained free of charge on application to CCDC, 12 Union Road, Cambridge CB2 1EZ, UK (fax: (+44)1223-336-033; e-mail: deposit@ccdc.cam.ac.uk).

## ■ AUTHOR INFORMATION


### Corresponding Author

*E-mail: t.hanusa@vanderbilt.edu (T.P.H.)

### Other Authors

E-mail: ross.f.koby@vanderbilt.edu (R.F. K.)

E-mail: nathan.schley@vanderbilt.edu (N. D. S.)

### ORCID

Ross F. Koby: 0000-0001-5394-1160

Timothy P. Hanusa: 0000-0002-7935-5968

Nathan D. Schley: 0000-0002-1539-6031


### Notes

The authors declare no competing financial interest

## ■ ACKNOWLEGEMENTS


Financial support by the National Science Foundation (CHE-1665327), the American Chemical Society–Petroleum Research Fund (56027-ND3), and a Charles M. Lukehart Fellowship (to RFK) is gratefully acknowledged. A reviewer is thanked for constructive comments.

## REFERENCES


1. In the broadest sense, a mechanochemical reaction is one induced by the direct absorption of mechanical energy. Such energy can be supplied in various forms, such as that from surface friction (tribology), sound (sonochemistry), shock waves, bond stretching (in macromolecular systems), and trituration (grinding and milling). The last form is under consideration here.
2. Tan, D.; Loots, L.; Friščić, T., Towards medicinal mechanochemistry: evolution of milling from pharmaceutical solid form screening to the synthesis of active pharmaceutical ingredients (APIs). *Chem. Commun.* **2016,** *52*, 7760-7781.
3. Andersen, J. M.; Mack, J., Decoupling the Arrhenius equation via mechanochemistry. *Chem. Sci.* **2017,** *8*, 5447-5453.
4. Hernández, J. G.; Bolm, C., Altering Product Selectivity by Mechanochemistry. *J. Org. Chem.* **2017,** *82*, 4007-4019.
5. Rightmire, N. R.; Hanusa, T. P.; Rheingold, A. L., Mechanochemical Synthesis of $[1,3\text{-}(SiMe_3)_2C_3H_3]_3$(Al,Sc), a Base-Free Tris(allyl)aluminum Complex and Its Scandium Analogue. *Organometallics* **2014,** *33*, 5952–5955.
6. Gečiauskaitė, A. A.; García, F., Main group mechanochemistry. *Beilstein J. Org. Chem.* **2017,** *13*, 2068-2077.
7. Wang, J.; Ganguly, R.; Yongxin, L.; Díaz, J.; Soo, H. S.; García, F., A multi-step solvent-free mechanochemical route to indium(III) complexes. *Dalton Trans.* **2016,** *45* (19), 7941-7946.
8. Glavinović, M.; Krause, M.; Yang, L.; McLeod, J. A.; Liu, L.; Baines, K. M.; Friščić, T.; Lumb, J.-P., A chlorine-free protocol for processing germanium. *Sci. Advan.* **2017,** *3*, e1700149.
9. Aleksanyan, D. V.; Churusova, S. G.; Aysin, R. R.; Klemenkova, Z. S.; Nelyubina, Y. V.; Kozlov, V. A., The first example of mechanochemical synthesis of organometallic pincer complexes. *Inorg. Chem. Commun.* **2017,** *76*, 33-35.
10. Jobbágy, C.; Tunyogi, T.; Pálinkás, G.; Deák, A., A Versatile Solvent-Free Mechanochemical Route to the Synthesis of Heterometallic Dicyanoaurate-Based Coordination Polymers. *Inorg. Chem.* **2011,** *50*, 7301-7308.
11. Jobbágy, C.; Molnar, M.; Baranyai, P.; Deák, A., Mechanochemical synthesis of crystalline and amorphous digold(I) helicates exhibiting anion- and phase-switchable luminescence properties. *Dalton Trans.* **2014,** *43*, 11807-11810.
12. Bowmaker, G. A.; Hanna, J. V.; Hart, R. D.; Healy, P. C.; King, S. P.; Marchetti, F.; Pettinari, C.; Skelton, B. W.; Tabacaru, A.; White, A. H., Mechanochemical and solution synthesis, X-ray structure and IR and $^{31}$P solid state NMR spectroscopic studies of copper(I) thiocyanate adducts with bulky monodentate tertiary phosphine ligands. *Dalton Trans.* **2012,** *41*, 7513-7525.
13. Garay, A. L.; Pichon, A.; James, S. L., Solvent-free synthesis of metal complexes. *Chem. Soc. Rev.* **2007,** *36*, 846-855.
14. Balaz, P.; Achimovicova, M.; Balaz, M.; Billik, P.; Cherkezova-Zheleva, Z.; Criado, J. M.; Delogu, F.; Dutkova, E.; Gaffet, E.; Gotor, F. J.; Kumar, R.; Mitov, I.; Rojac, T.; Senna, M.; Streletskii, A.; Wieczorek-Ciurowa, K., Hallmarks of mechanochemistry: from nanoparticles to technology. *Chem. Soc. Rev.* **2013,** *42*, 7571-7637.
15. Baláž, P., *Mechanochemistry in Nanoscience and Minerals Engineering*. Springer: 2008.
16. Anastas, P. T.; Warner, J. C., *Green Chemistry: Theory and Practice*. Oxford University Press: New York, 1998.
17. Li, C.-J.; Anastas, P. T., Green Chemistry: present and future. *Chem. Soc. Rev.* **2012,** *41*, 1413-1414.
18. Shi, Y. X.; Xu, K.; Clegg, J. K.; Ganguly, R.; Hirao, H.; Friščić, T.; García, F., The First Synthesis of the Sterically Encumbered Adamantoid Phosphazane $P_4(N^tBu)_6$: Enabled by Mechanochemistry. *Angew. Chem. Int. Ed.* **2016,** *55*, 12736-12740.
19. Komatsu, K.; Wang, G.-W.; Murata, Y.; Tanaka, T.; Fujiwara, K.; Yamamoto, K.; Saunders, M., Mechanochemical Synthesis and Characterization of the Fullerene Dimer $C_{120}$. *J. Org. Chem.* **1998,** *63*, 9358-9366.
20. Zhu, S.-E.; Li, F.; Wang, G.-W., Mechanochemistry of fullerenes and related materials. *Chem. Soc. Rev.* **2013,** *42*, 7535-7570.
21. $[SnMe_4]$ decomposes above 400 °C, for example, but its mean bond enthalpy $\bar{D}$(Sn–C) is only 52 kcal mol$^{-1}$ (Elschenbroich, C. *Organometallics*, VCH Publishers, Weinheim, 3rd ed., 2006, p. 16).
22. Davidson, P. J.; Harris, D. H.; Lappert, M. F., The synthesis and physical properties of kinetically stable bis(bistrimethsilylmethyl)Ge(II), Sn(II), and Pb(II). *J. Chem. Soc., Dalton Trans.* **1976**, 2268-2274.
23. Jutzi, P.; Burford, N., Structurally diverse π-Cp complexes of the Main Group elements. *Chem. Rev.* **1999,** *99*, 969-990.
24. Becerra, R.; Gaspar, P. P.; Harrington, C. R.; Leigh, W. J.; Vargas-Baca, I.; Walsh, R.; Zhou, D., Direct Detection of Dimethylstannylene and Tetramethyldistannene in Solution and the Gas Phase by Laser Flash Photolysis of 1,1-Dimethylstannacyclopent-3-enes. *J. Am. Chem. Soc.* **2005,** *127*, 17469-17478.
25. Hanusa, T. P.; Carlson, C. N., Transition Metal Complexes with Bulky Allyl Ligands. In *Encyclopedia of Inorg. Chem.-II*, King, R. B., Ed. Wiley: 2005; Vol. 9, pp 5690–5695.
26. Chmely, S. C.; Hanusa, T. P., Complexes with Sterically Bulky Allyl Ligands: Insights into Structure and Bonding. *Eur. J. Inorg. Chem.* **2010**, 1321-1337.
27. Solomon, S. A.; Layfield, R. A., The coordination chemistry of silyl-substituted allyl ligands. *Dalton Trans.* **2010,** *39*, 2469-2483.
28. Layfield, R. A.; García, F.; Hannauer, J.; Humphrey, S. M., Ansa-tris(allyl) complexes of alkali metals: Tripodal analogues of cyclopentadienyl and ansa-metallocene ligands. *Chem. Commun.* **2007**, 5081-5083.
29. Boyde, N.; Rightmire, N.; Hanusa, T.; Brennessel, W., Symmetric Assembly of a Sterically Encumbered Allyl Complex: Mechanochemical and Solution Synthesis of the Tris(allyl)beryllate, $K[BeA'_3]$ (A' = 1,3-$(SiMe_3)_2C_3H_3$). *Inorganics* **2017,** *5* (2), 36.
30. Gren, C. K.; Hanusa, T. P.; Rheingold, A. L., Threefold Cation–π Bonding in Trimethylsilylated Allyl Complexes. *Organometallics* **2007,** *26*, 1643–1649.
31. Rightmire, N. R.; Bruns, D. L.; Hanusa, T. P.; Brennessel, W. W., Mechanochemical Influence on the Stereoselectivity of Halide Metathesis: Synthesis of Group 15 Tris(allyl) Complexes. *Organometallics* **2016,** *35*, 1698–1706.
32. Monomeric $[SnA'_2]$ is calculated to be a minimum on its potential energy surface at the B3PW91-D3BJ/def2-TZVPD level. The dissociation step of $(SnA'_2 \rightarrow \bullet SnA' + \bullet A')$ is estimated at 36.8 kcal mol$^{-1}$ ($\Delta H°$; $\Delta G° = 22.1$ kcal mol$^{-1}$). Of course, were $[SnA'_2]$ to be generated, it might well exist in the form of a coordination polymer with different energetics. See SI for geometry-optimized coordinates. .
33. Kleeberg, C.; Grunenberg, J.; Xie, X., K–$H_3C$ and K–Sn Interactions in Potassium Trimethylstannyl Complexes: A Structural, Mechanochemical, and NMR Study. *Inorg. Chem.* **2014,** *53*, 4400-4410.
34. Shannon, R. D., Revised effective ionic radii and systematic studies of interatomic distances in halides and chalcogenides. *Acta Crystallogr., Sect A* **1976,** *32*, 751-767.
35. Milled KCl typically has a pale bluish-gray apperance, visibly distinct from the tin remaining after the formation of the Sn(IV)-contaning **3**. As a check on the presence of other tin species, a $^{119}$Sn NMR spectrum was taken of the powder placed in $C_6D_6$; no signal was observed from δ +500 to -2000 ppm.
36. Quisenberry, K. T.; Smith, J. D.; Voehler, M.; Stec, D. F.; Hanusa, T. P.; Brennessel, W. W., Trimethylsilylated Allyl Complexes of Nickel. The Stabilized Bis(π-allyl)nickel Complex $[\eta^3\text{-}1,3\text{-}(SiMe_3)_2C_3H_3]_2Ni$ and its Mono(π-allyl)NiX (X = Br, I) Derivatives. *J. Am. Chem. Soc.* **2005,** *127*, 4376-4387.
37. Wrackmeyer, B., NMR Spectroscopy of Tin Compounds. In *Tin Chemistry: Fundamentals, Frontiers, and Applications*, Davies, A. G.; Gielen, M.; Pannell, K. H.; Tiekink, E. R. T., Eds. John Wiley & Co,: Chichester, 2008; pp 17-52.
38. Hernández, J. G.; Butler, I. S.; Friščić, T., Multi-step and multi-component organometallic synthesis in one pot using orthogonal mechanochemical reactions. *Chem. Sci.* **2014,** *5*, 3576-3582.
39. Hernández, J. G.; Macdonald, N. A. J.; Mottillo, C.; Butler, I. S.; Friščić, T., A mechanochemical strategy for oxidative addition: remarkable yields and stereoselectivity in the halogenation of organometallic Re(I) complexes. *Green Chem.* **2014,** *16*, 1087-1092.
40. Brown, P.; Mahon, M. F.; Molloy, K. C., Sterically hindered organotin compounds. Part 1. Synthesis and reaction chemistry of tris(trimethylsilyl)methyltin(IV) derivatives. X-Ray crystal structures of $Sn(CH_2Ph)_2[C(SiMe_3)_3](OSiMe_3)$ and $Sn(CH_2Ph)_2[C(SiMe_3)_3]\text{-}[CH_2CH{=}C(SiMe_3)_2]$. *J. Chem. Soc., Dalton Trans.* **1990**, 2643-2651.
41. Friščić, T.; Halasz, I.; Beldon, P. J.; Belenguer, A. M.; Adams, F.; Kimber, S. A. J.; Honkimäki, V.; Dinnebier, R. E., Real-time and in situ monitoring of mechanochemical milling reactions. *Nat. Chem.* **2012,** *5*, 66-73.
42. Halasz, I.; Kimber, S. A. J.; Beldon, P. J.; Belenguer, A. M.; Adams, F.; Honkimäki, V.; Nightingale, R. C.; Dinnebier, R. E.; Friščić, T., In situ and

real-time monitoring of mechanochemical milling reactions using synchrotron X-ray diffraction. *Nat. Protoc.* **2013,** *8*, 1718-1729.
43. Kulla, H.; Fischer, F.; Benemann, S.; Rademann, K.; Emmerling, F., The effect of the ball to reactant ratio on mechanochemical reaction times studied by in situ PXRD. *CrystEngComm* **2017,** *19*, 3902-3907.
44. Gracin, D.; Štrukil, V.; Friščić, T.; Halasz, I.; Užarević, K., Laboratory Real-Time and In Situ Monitoring of Mechanochemical Milling Reactions by Raman Spectroscopy. *Angew. Chem. Int. Ed.* **2014,** *53* (24), 6193-6197.
45. Juribašić, M.; Užarević, K.; Gracin, D.; Ćurić, M., Mechanochemical C-H bond activation: rapid and regioselective double cyclopalladation monitored by in situ Raman spectroscopy. *Chem. Commun.* **2014,** *50*, 10287-10290.
46. Štrukil, V.; Gracin, D.; Magdysyuk, O. V.; Dinnebier, R. E.; Friščić, T., Trapping Reactive Intermediates by Mechanochemistry: Elusive Aryl N-Thiocarbamoylbenzotriazoles as Bench-Stable Reagents. *Angew. Chem. Int. Ed.* **2015,** *54*, 8440-8443.
47. Fischer, F.; Fendel, N.; Greiser, S.; Rademann, K.; Emmerling, F., Impact Is Important—Systematic Investigation of the Influence of Milling Balls in Mechanochemical Reactions. *Org. Process Res. Dev.* **2017,** *21*, 655-659.
48. Užarević, K.; Halasz, I.; Friščić, T., Real-Time and In Situ Monitoring of Mechanochemical Reactions: A New Playground for All Chemists. *J. Phys. Chem. Lett.* **2015,** *6*, 4129-4140.
49. Lukin, S.; Stolar, T.; Tireli, M.; Blanco, M. V.; Babić, D.; Friščić, T.; Užarević, K.; Halasz, I., Tandem In Situ Monitoring for Quantitative Assessment of Mechanochemical Reactions Involving Structurally Unknown Phases. *Chem – Eur. J.* **2017,** *23*, 13941-13949.
50. Prince, R. H., Reaction mechanism in organometallic compounds. Comparative solvolyses of organotin and organosilicon chlorides. *J. Chem. Soc.* **1959**, 1783-1790.
51. The B3PW91 functional incorporates Becke's 3-parameter exchange functional (Becke, A. D. *J. Chem. Phys.*, 1993, **98**, 5648-5652) and the Perdew-Wang gradient corrected correlation functional (K. Burke, K; Perdew, J. P.; Wang, Y., in *Electronic Density Functional Theory: Recent Progress and New Directions*, Ed. J. F. Dobson, G. Vignale, and M. P. Das (Plenum, 1998).
52. Grimme, S.; Antony, J.; Ehrlich, S.; Krieg, H., A consistent and accurate ab initio parametrization of density functional dispersion correction (DFT-D) for the 94 elements H-Pu. *J. Chem. Phys.* **2010,** *132*, 154104/1-154104/19.
53. Grimme, S.; Ehrlich, S.; Goerigk, L., Effect of the damping function in dispersion corrected density functional theory. *J. Comput. Chem.* **2011,** *32*, 1456-1465.
54. Scott, W. J.; Moretto, A. F., Tetraallylstannane. In *e-EROS Encyclopedia of Reagents for Organic Synthesis*, John Wiley & Sons, Ltd.: 2001; pp 1-2.
55. Pereyre, M.; Quintard, J.-P.; Rahm, A., Tin in Organic Synthesis. Butterworths: London, 1987; p 342.
56. Davies, A. G., Allyl-, Allenyl-, Propargyl-, and Cyclopentadienyl-stannanes. In *Organotin Chemistry*, 2 ed.; Wiley-VCH: Weinheim, 2004; p 135.
57. Kawakami, K.; Kuivila, H. G., Preparation and spectral characteristics of some allyltins. Nature of allyltin interactions. *J. Org. Chem.* **1969,** *34*, 1502-1504.
58. Ulrich, W.; Armin, S., Nature of the "Silicon β-Effect" in Allyltrimethylsilane. *Angew. Chem. Int. Ed. Engl.* **1972,** *11*, 146-147.
59. Burshtein, K. Y.; Isaev, A. N.; Shorygin, P. P., σ-π Interaction in some σ-bonded allyl compounds. A MNDO study. *J. Organomet. Chem.* **1989,** *361*, 21-25.
60. Bach, R. D.; Scherr, P. A., Extended Hückel calculations on group IV allyl compounds evidence for σ-π conjugation. *Tetrahedron Lett.* **1973,** *14*, 1099-1102.
61. Mayer, I., Charge, bond order and valence in the AB initio SCF theory. *Chem Phys. Lett.* **1983,** *97*, 270-274.
62. Bridgeman, A. J.; Cavigliasso, G.; Ireland, L. R.; Rothery, J., The Mayer bond order as a tool in inorganic chemistry. *J. Chem. Soc., Dalton Trans.* **2001**, 2095-2108.
63. Simões, J. A. M., Organometallic Thermochemistry Data. In *NIST Chemistry WebBook, NIST Standard Reference Database Number 69*, Linstrom, P. J.; Mallard, W. G., Eds. National Institute of Standards and Technology: Gaithersburg MD, 2018. DOI: 10.18434/T4D303
64. The first dissociation energy is typically appreciably higher than the second and subsequent steps for many main group homoleptic alkyls (see ref. 21).
65. Guzei, I. A.; Wendt, M., An improved method for the computation of ligand steric effects based on solid angles. *Dalton Trans.* **2006**, 3991-3999.
66. Values of $G_{complex}$ that approach 100% are associated with molecules that display strucural evidence of steric strain. including bond lengthening (and presumably weakening). See ref. 65 for examples.
67. Grimme, S.; Huenerbein, R.; Ehrlich, S., On the Importance of the Dispersion Energy for the Thermodynamic Stability of Molecules. *ChemPhysChem* **2011,** *12*, 1258-1261.
68. Kahr, B.; Van Engen, D.; Mislow, K., Length of the ethane bond in hexaphenylethane and its derivatives. *J. Am. Chem. Soc.* **1986,** *108*, 8305-8307.
69. Grimme, S.; Schreiner, P. R., Steric Crowding Can Stabilize a Labile Molecule: Solving the Hexaphenylethane Riddle. *Angew. Chem. Int. Ed.* **2011,** *50*, 12639-12642.
70. Liptrot, D. J.; Power, P. P., London dispersion forces in sterically crowded inorganic and organometallic molecules. *Nat. Rev. Chem.* **2017,** *1*, 0004.
71. Bondi, A., van der Waals Volumes and Radii. *J. Phys. Chem.* **1964,** *68*, 441-451.
72. Gamsjäger, H.; Gajda, T. s.; Saxena, S. K.; Sangster, J.; Voigt, W., *Chemical Thermodynamics of Tin*. OECD Nuclear Energy Agency: Paris, France, 2012; Vol. 12.
73. Čerič, B.; Bukovec, P., Thermal decomposition of the mixture of antimony(III) oxide and tin(II) chloride. *Thermochim. Acta* **1992,** *195*, 73-84.
74. $SnCl_2$ is a white, air-stable solid (mp 246 °C); $SnCl_4$ is a hygroscopic liquid (mp -33 °C) that fumes on contact with air. The ground sample of $SnCl_2$ was unchanged in appearance; there was no darkening, as would be the case if elemental tin had formed, no liquid was present, and the solid was not noticeably clumped together, as might have occurred as a result of partial formation of $SnCl_4$. There was no visible evidence of any fuming when the ground powder was exposed to air.

Insert Table of Contents artwork here